Planta
DOI 10.1007/s00425-017-2681-0

ORIGINAL ARTICLE

Virus-induced gene silencing of the two squalene synthase isoforms of apple tree (*Malus* × *domestica* L.) negatively impacts phytosterol biosynthesis, plastid pigmentation and leaf growth

Sandra M. Navarro Gallón[1,2] · Carolina Elejalde-Palmett[1] · Dimitri Daudu[1] · Franziska Liesecke[1] · Frédéric Jullien[3] · Nicolas Papon[4] · Thomas Dugé de Bernonville[1] · Vincent Courdavault[1] · Arnaud Lanoue[1] · Audrey Oudin[1] · Gaëlle Glévarec[1] · Olivier Pichon[1] · Marc Clastre[1] · Benoit St-Pierre[1] · Lucia Atehortùa[2] · Nobuyuki Yoshikawa[5] · Nathalie Giglioli-Guivarc'h[1] · Sébastien Besseau[1]

Received: 20 January 2017 / Accepted: 17 March 2017

Abstract

Main conclusion **The use of a VIGS approach to silence the newly characterized apple tree SQS isoforms points out the biological function of phytosterols in plastid pigmentation and leaf development.**

Triterpenoids are beneficial health compounds highly accumulated in apple; however, their metabolic regulation is poorly understood. Squalene synthase (SQS) is a key branch point enzyme involved in both phytosterol and triterpene biosynthesis. In this study, two SQS isoforms were identified in apple tree genome. Both isoforms are located at the endoplasmic reticulum surface and were demonstrated to be functional SQS enzymes using an in vitro activity assay. Md*SQS1* and Md*SQS2* display specificities in their expression profiles with respect to plant organs and environmental constraints. This indicates a possible preferential involvement of each isoform in phytosterol and/or triterpene metabolic pathways as further argued using RNAseq metatranscriptomic analyses. Finally, a virus-induced gene silencing (VIGS) approach was used to silence Md*SQS1* and Md*SQS2*. The concomitant down-regulation of both MdSQS isoforms strongly affected phytosterol synthesis without alteration in triterpene accumulation, since triterpene-specific oxidosqualene synthases were found to be up-regulated to compensate metabolic flux reduction. Phytosterol deficiencies in silenced plants clearly disturbed chloroplast pigmentation and led to abnormal development impacting leaf division rather than elongation or differentiation. In conclusion, beyond the characterization of two SQS isoforms in apple tree, this work brings clues for a specific involvement of each isoform in phytosterol and triterpene pathways and emphasizes the biological function of phytosterols in development and chloroplast integrity. Our report also opens the door to metabolism studies in *Malus domestica* using the apple latent spherical virus-based VIGS method.

Keywords Apple latent spherical virus (ALSV) · Apple tree · Phytosterol · Squalene synthase · Triterpene · VIGS

Abbreviations

ALSV	Apple latent spherical virus
CAS	Cycloartenol synthase
SQS	Squalene synthase
FPP	Farnesyl diphosphate
OSC	Oxidosqualene cyclase
VIGS	Virus-induced gene silencing

Electronic supplementary material The online version of this article (doi:10.1007/s00425-017-2681-0) contains supplementary material, which is available to authorized users.

Sandra M. Navarro Gallón and Carolina Elejalde-Palmett contributed equally to this work.

✉ Sébastien Besseau
sebastien.besseau@univ-tours.fr

[1] EA2106 Biomolécules et Biotechnologies Végétales, Université François Rabelais de Tours, Tours, France

[2] Laboratorio de Biotecnologia, Sede de Investigacion Universitaria, Universidad de Antioquia, Medellin, Colombia

[3] EA3061 Laboratoire de Biotechnologies Végétales appliquées aux plantes aromatiques et médicinales, Université Jean Monnet de Saint Etienne, Saint Etienne, France

[4] EA3142 Groupe d'Etude des Interactions Hôte-Pathogène, Université d'Angers, Angers, France

[5] Plant Pathology Laboratory, Iwate University, Morioka, Japan

Published online: 27 March 2017

Introduction

Squalene synthase (SQS) catalyzes the first enzymatic step of triterpenoid biosynthesis which are lipophilic C30-derivative terpenes, ubiquitously produced in animals, fungus and plants. SQS condenses two farnesyl diphosphates (FPP) to produce squalene. This reaction is followed by an oxidative step catalyzed by the squalene epoxidase (SQE) yielding 2,3 oxidosqualene. This reactive intermediate is further diversely cyclized by a large family of oxidosqualene cyclases (OSC) (Fig. 1). Depending on specific carbocation rearrangements catalyzed by OSC, wide series of triterpenoid skeletons can be generated. In plants, the most widespread triterpenoid forms are phytosterols (i.e., tetracyclic triterpenoids) and triterpenes (i.e., pentacyclic triterpenoids). Sterols are produced in all eukaryotic organisms and are currently considered as essential compounds. Their synthesis involved OSC that cyclize 2,3 oxidosqualene in a chair–boat–chair conformation with a protosteryl cation intermediate (Phillips et al. 2006). In mammals and fungi, lanosterol synthase (LAS) (Shi et al. 1994; Baker et al. 1995) leads to lanosterol, further converted into cholesterol and ergosterol as main compounds, respectively, whereas in plants, cycloartenol synthase (CAS) (Corey et al. 1993) is the entry point for the synthesis of a mixture of sterols, the so-called phytosterols (Fig. 1), composed of β-sitosterol, stigmasterol and campesterol as predominant forms (Benveniste 2002). However, the existence of an additional minor branch to produce cholesterol in some plants can be noticed (Kolesnikova et al. 2006; Suzuki et al. 2006; Sonawane et al. 2016). Sterols are important membrane structural components, impacting fluidity and impermeability (Hartmann 1998). Beside this function, sterols participate in plant development and defense regulation (Lindsey et al. 2003) notably through brassinosteroids which are plant-specific steroid hormones produced from campesterol (Wang et al. 2014) (Fig. 1). Triterpenes are a large class of plant natural products. Their synthesis also involves distinct OSC cyclizing 2,3 oxidosqualene in a chair–chair–chair conformation with a dammarenyl cation intermediate (Phillips et al. 2006). β-Amyrin synthase (β-AS) (Kushiro et al. 1998), α-amyrin synthase (α-AS) (Brendolise et al. 2011) and lupeol synthase (LUP) (Herrera et al. 1998) are the main representative triterpene synthases leading, respectively, to the common oleanane, ursane and lupane-type triterpenes (Fig. 1). These compounds belong to specialized membranes and are usually reported in higher amounts in cuticular waxes (Bringe et al. 2006; Jäger et al. 2009; Wang et al. 2011; Racovita and Jetter 2016), providing protective function against insect and microbial attacks (González-Coloma et al. 2011). Finally, triterpenes can be glycosylated and referred to as saponins (Vincken et al. 2007).

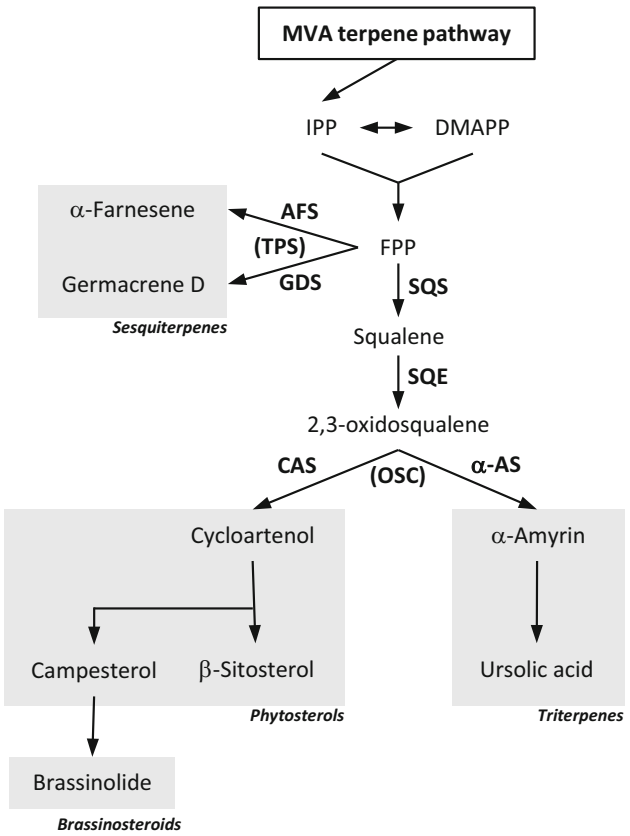

Fig. 1 Simplified mevalonate-derived terpene biosynthesis pathway leading to sesquiterpenes, triterpenes, phytosterols and brassinosteroids. Main compounds found to accumulate in apple tree are indicated for each terpene family. Enzymes found in several plants to be involved in primary steps are mentioned. *IPP* isopentenyl pyrophosphate, *DMAPP* dimethylallyl pyrophosphate, *FPP* farnesyl pyrophosphate, *SQS* squalene synthase, *SQE* squalene epoxidase, *AFS* α-farnesene synthase, *GDS* germacrene D synthase, *CAS* cycloartenol synthase, *α-AS* α-amyrin synthase, *TPSs* terpene synthases (e.g., GDS and AFS), *OSC* oxidosqualene cyclases (e.g., CAS and α-AS)

SQS are endoplasmic reticulum (ER) bound enzymes with a cytosolic catalytic domain catalyzing the synthesis of squalene in a two consecutive steps reaction. First, presqualene diphosphate is generated by the condensation of two FPP, followed by a reduction reaction implying NADPH as co-factor. SQS genes were first cloned and studied in yeast (Jennings et al. 1991) and mammals (Mckenzie et al. 1992; Summers et al. 1993). Thereafter, the enzyme was characterized in plants revealing the conservation of the three catalytic domains (A, B and C-domains) previously identified in rat by mutagenesis studies (Gu et al. 1998) and in human through crystal structure determination (Pandit et al. 2000). However, SQS greatly differs between kingdoms in their C-terminal end which contains the transmembrane domain allowing ER anchoring. In higher plants, SQS cDNA was cloned and studied in plethora of plants; however, information on gene

copy numbers is patchy. To date, *SQS* gene was reported either as single copy gene like in mammals and yeast or as a small gene family, as well. A single *SQS* gene was identified in genomes of rice (Hata et al. 1997), *Taxus cuspidata* (Huang et al. 2007) and *Euphorbia tirucalli* (Uchida et al. 2009). Two genes were found in tobacco (Devarenne et al. 1998), *Glycyrrhiza glabra* (Hayashi et al. 1999) *Medicago truncatula* (Suzuki et al. 2002) and *Arabidopsis thaliana* albeit one seems to be a pseudogene (Busquets et al. 2008). Finally, in *Panax ginseng* up to three *SQS* copies were functionally characterized (Kim et al. 2011). SQS constitutes a rate-limiting enzyme for triterpenoid synthesis as demonstrated by sterols and triterpene saponins accumulation in SQS-overexpressed lines of *P. ginseng* and *Eleutherococcus senticosus* (Lee et al. 2004; Seo et al. 2005). Therefore, regulation of SQS ensures a fine-tuned control of metabolic fluxes through the triterpenoid metabolism; however, the function of SQS for squalene distribution in subsequent branches of the pathway remains unclear. For instance, a fungal elicitor treatment on parsley and tobacco cell cultures led to a concomitant decrease in SQS activity and sterol biosynthesis, allowing FPP substrates to be rerouted to sesquiterpene synthesis as plant defense response metabolites (Vögeli and Chappell 1988; Haudenschild and Hartmann 1995; Devarenne et al. 1998). Interestingly, the regulation of SQS activity was observed with only minor transcript variations suggesting an important post-translational regulation of the enzyme (Devarenne et al. 1998). Finally, additional regulations occur independently between phytosterol and triterpene metabolisms at several other enzymatic steps along the pathways (Schaller 2004).

Consumption of apple has been proven beneficial to human health. The apple tree polyphenol metabolism mainly participates to this property by ensuring a significant production of dihydrochalcones (Dugé de Bernonville et al. 2010) and flavonoids (Eberhardt et al. 2000). However, triterpenoids produced in apple also present interesting nutritional and pharmacologic virtues. For instance, apple tree triterpene extracts were found to display radical scavenging activities and an antiproliferative potential against tumor cells (D'Abrosca et al. 2005; Ma et al. 2005; He and Rui 2007). The availability of the apple tree genome sequence (Velasco et al. 2010) has progressively promoted the identification of enzymes involved in the biosynthesis of triterpenes and sesquiterpenes. Up to now, ten terpene synthases (TPS, Fig. 1) and five OSC (Fig. 1) were characterized in this species (Pechous and Whitaker 2004; Brendolise et al. 2011; Nieuwenhuizen et al. 2013; Andre et al. 2016). Among them, MdOSC1 and MdOSC3 were shown to be α-amyrin synthase, allowing the accumulation of ursolic acid as the main apple tree triterpene (Brendolise et al. 2011). In a continuing effort to elucidate the apple tree sterol and triterpene biosynthetic pathways, we were herein particularly interested in identifying and characterizing *SQS* genes as well as deciphering their physiological roles in planta. Two functional and differentially expressed SQS isoforms were identified. By taking advantage of a virus-induced gene silencing (VIGS) method, we demonstrated the crucial role of SQS in phytosterol synthesis and their importance in leaf development and plastid pigmentation in apple tree.

Materials and methods

Plant material and growth conditions

Seeds of *Malus domestica* cultivar 'Golden Delicious' (provided by INRA d'Angers, France) were vernalized 3 months in wet vermiculite at 4 °C. Plants were grown in a greenhouse at 21 °C with 50% relative humidity and under a light/dark cycle of 14/10 h. Apple tree materials were collected on 2-month-old plants except for flowers collected on mature trees in orchards. Cold and osmotic stresses were performed on 5-week-old plants. For cold treatment, plants were grown at 4 °C with light cycle. To induce osmotic stress, soil was watered and saturated with 15% PEG-6000.

Sequence alignment and phylogeny analysis

Previously characterized At*SQS1*, At*SQS2* (*A. thaliana*), Mo*SQS* (*Magnolia officinalis*), Nt*SQS* (*Nicotiana tabacum*), Pg*SS1* (*P. ginseng*) and Lj*SqS* (*Lotus japonicus*) sequences were used as queries for BLASTN searches in the apple tree genome (Velasco et al. 2010) using the phytozome database (Goodstein et al. 2012). Corresponding protein sequences were aligned with ClustalX (v2.0.11) and the resulting alignment was used to construct a neighbor-joining phylogenetic tree with bootstrap non-parametric resampling procedure.

Isolation of SQS genes

Md*SQS1* and Md*SQS2* ORFs were amplified with Phusion high-fidelity DNA polymerase (Fermentas) from leaf cDNA using the same couple of primers (MdSQSFwd and MdSQSRev; Suppl. Table S1). PCR products were further cloned in pGEM-T easy vector (Promega). Sequencing of positive clones discriminated Md*SQS1* and Md*SQS2* sequences which were submitted in NCBI database (accession numbers KC895979 and KC895980). *Saccharomyces cerevisiae ERG9* (Sc*ERG9*) was cloned in pGEM-T easy using yeast gDNA and specific primers

(ScERG9Fwd and ScERG9Rev; Suppl. Table S1). Finally, chimeric MdSQS1^{ScTM} and MdSQS2^{ScTM}, in which the C-terminal region of apple tree SQS (residues 316–412 and 316–410, respectively, for MdSQS1 and MdSQS2) was replaced by the equivalent region of ScERG9 (residues 326–444), were generated by PCR overlap extension method (Ho et al. 1989) and cloned in pGEM-T easy vector. PCRs were performed using external primer (MdSQSFwd or ScERG9Rev) and overlap internal primer (MdSQSwoTMRev or ScERG9TMFwd; Suppl. Table S1).

Yeast complementation experiments

For yeast complementation assays, Md*SQS1*, Md*SQS2*, Md*SQS1*^{ScTM}, Md*SQS2*^{ScTM} and Sc*ERG9* were amplified from sequences sub-cloned in pGEM-T easy vector, using specific primers containing BamHI and XhoI restriction sites (Suppl. Table S1) and cloned in pYES2.0 yeast expression vector under the inducible *GAL1* gene promoter. Plasmids were integrated in the *S. cerevisiae erg9* mutant strain 2C1 (provided by Marc Fischer) following a standard electroporation procedure (Becker and Guarente 1991). Cells were selected on CSM-URA plates (0.8% yeast nitrogen base w/o amino acids, 2% glucose and dropout mix-URA) complemented with 80 µg/ml ergosterol (in tergitol NP-40/ethanol, 1:1, v/v). After 5 days at 30 °C, transformed yeasts were plated on YPGal medium (2% bacto peptone, 1% yeast extract and 2% galactose) to induce recombinant protein expression in strain 2C1 (Kribii et al. 1997).

Enzyme assay

Saccharomyces cerevisiae erg9 mutant strain 2C1 harboring expressing vectors were grown in liquid medium complemented with 4 µg/ml ergosterol, 2 days at 30 °C in CSM-URA and followed by an additional 12 h culture at 30 °C in YPGal medium to induce recombinant protein expression. Cells were harvested and mechanically lysed with acid-washed glass beads in 50 mM Tris–HCl buffer, pH 7.5, containing 1 mM EDTA, 600 mM sorbitol, 1 mM DTT, 1 mM PMSF. Crude extracts were directly used for enzymatic assays. The SQS activity was measured in 100 µl volume reaction containing 50 mM Tris–HCl buffer (pH 7.5), 5 mM $MgCl_2$, 2 mM β-mercaptoethanol, 50 µM FPP and 3 mM NADPH. After 30 min at 35 °C, reaction products were extracted three times with two volumes of hexane and concentrated under nitrogen flux. Samples were analyzed by TLC on silica gel 60, developed in hexane/chloroform (9:1, v/v) and colored with iodine vapor. Authentic squalene was used as standard (Sigma-Aldrich).

Subcellular localization studies

The full-length coding sequences of Md*SQS1* and Md*SQS2* were amplified with specific primers containing SpeI restriction sites (Suppl. Table S1) and cloned in the pSCA-YFP vector in frame with the 3′-end of the YFP coding sequence. *Catharanthus roseus* C20D cells were transiently transformed with the resulting pSCA-YFP constructs in combination with the endoplasmic reticulum (ER)-CFP marker (Nelson et al. 2007), using particle bombardment as described by (Guirimand et al. 2009). Briefly, *C. roseus* plated cells were bombarded with DNA-coated gold particles (1 µm) and 1100 psi rupture disc at a stopping-screen-to-target distance of 6 cm, using the Bio-Rad PDS1000/He system. Cells were cultivated for 16–38 h before being harvested and observed. The subcellular localization was determined using an Olympus BX-51 epifluorescence microscope equipped with an Olympus DP-71 digital camera and a combination of YFP and CFP filters. The pattern of localization presented in this work is representative of circa 50 observed cells.

Gene expression analysis

Extractions of total RNA were performed using the NucleoSpin RNA kit (Macherey-Nagel), with an improved extraction protocol (Elejalde-Palmett et al. 2015). First-strand cDNA were synthesized from 1 µg of total RNA using oligo(dT)18 and RevertAid Reverse Transcriptase (Fermentas) according to the manufacturer's instructions. Quantitative PCR analysis were performed on a CFX96 Touch Real-Time PCR System (Bio-Rad). Each PCR of 15 µl contains equal amount of cDNA, 1× DyNAmo SYBR Green mix (Fermentas) and specific primers for each genes, except for Md*SQS1* and Md*SQS2* transcripts which were commonly amplified (Suppl. Table S1). Amplification was initiated by a denaturation step at 95 °C for 10 min followed by 40 cycles at 95 °C for 15 s and 60 °C for 30 s. Melting curves were used to determine the specificity of reactions. Calibration curves were made for each couple of primers to ensure PCR efficiency and performed absolute quantification when needed. Otherwise, relative quantification of gene expression was calculated according to the $\Delta\Delta C_t$ method. Md*EF1alpha* was used as reference gene. Each assay was performed in duplicate and expression measurements were achieved at least twice with independent biological repetitions. Since Md*SQS1* and Md*SQS2* transcripts cannot be distinguished with the primers used for qPCR, expression ratio of each transcript among total *SQS* transcripts amplified was measured (Suppl. Fig. S1). For this purpose, cDNA were pre-amplified using Phusion DNA polymerase and MdSQS primers during six cycles. Pre-amplicons were divided into four equivalent tubes and subjected to digestion with *Dra*I, *Psi*I, both or none (fast digest enzymes;

Fermentas). Further qPCR was done with MdSQS primers in classical conditions. *Dra*I restriction site was found in Md*SQS1* amplicon but not for Md*SQS2*, and inversely for *Psi*I. Consequently, *SQS* transcript ratios were calculated with *SQS* copy numbers obtained in single digested pre-amplicons compared to undigested and normalized with Md*EF1alpha*.

RNA-seq data analysis

A total of 417 raw RNAseq data for *M. domestica* were downloaded from EBI as fastq files (Suppl. Table S2). Gene expression was quantified by pseudo-aligning reads on *M. domestica* reference transcripts v3.0 with Salmon v0.7.2 (Patro et al. 2016) using the variational Bayesian Expectation–Maximization algorithm and sequence bias correction to improve quantification. A total of 310 samples where more than 50% of the reads pseudo-aligned were kept. Linear correlations between transcript expression levels (TPM, transcript per million) were calculated with the Pearson Correlation Coefficient, which were subsequently used to determine the Highest Reciprocal Ranks (HRR) between each pair of transcripts (Mutwil et al. 2011). This ranking procedure is expected to be more integrative than the two-dimension PCC as it takes into account the PCC of all other genes for each pair. Transcripts were considered to be co-expressed with MdSQS1 or MdSQS2 when the HRR was below 2,000 (Suppl. Table S3).

Annotation of *M. domestica* transcripts was performed as described in Zhang et al. (2015) with the Trinotate pipeline. Candidate triterpene and phytosterol-related genes were obtained from the Gene Ontology (GO) annotation associated with Uniprot entries using "triterpenoid" and "steroid biosynthetic process" search terms (Suppl. Table S4). Average expression profiles of candidate genes from the two classes were obtained over the 310 samples and visualized within R and the ggplot2 package (R Core Team 2015). To improve readability, expression profiles were smoothed with a generalized additive model including a 99% confidence interval.

VIGS experiments

Virus-induced gene silencing technology was used to induce *SQS* gene silencing in apple tree with the apple latent spherical virus (ALSV) system (Sasaki et al. 2011). A 201pb fragment of Md*SQS1* and *rbcS* coding sequence were amplified (Suppl. Fig. S2 and Suppl. Table S1) and cloned into XhoI and BamHI sites of vector pEALSR2L5R5. The resulting plasmids, combined with pEALSR1, were used to produce virus in *Chenopodium quinoa*. Virus RNA were used for apple tree seedlings transformation by biolistic as described by (Sasaki et al. 2011).

Histochemical analysis

Apple tree leaves were fixed with a solution containing 3.7% formaldehyde, 50% ethanol, and 5% acetic acid in water, dehydrated in an ethanol series, transferred to ter-butanol, and gradually embedded in paraplast. Transverse sections (10 µm thick) were made with a Leica RM2125 RTS microtome. Paraplast was removed with xylene; leaf cross sections were then rehydrated, stained with 0.5% astra blue for 5 min, rinsed, dehydrated in ethanol series, and mounted on slides with Eukitt. Observations were done with an Olympus BX51 microscope. Cell size was measured with Cell D software.

Terpene extraction and analysis

Sesquiterpenes of apple leaves were extracted by hexane (4 ml/gFW) with camphor as internal standard (1 mg/l). Injection volume was 2 µl in split 1:2 mode on an Agilent GC 6850 gas chromatograph coupled with an Agilent 5973 ion trap mass detector. The instrument was equipped with a 30 m × 0.25 mm DB5 apolar capillary column. Temperatures of injector and detector were 250 °C. Helium was used as the carrier gas at a flow rate of 1.0 ml/min. Oven temperature settings were: 60 °C at injection followed by a 3 °C/min temperature ramp from 60 to 150 °C, then 7 °C/min from 150 to 240 °C. Temperature was then kept on hold at 240 °C for 5 min. Molecule identification was performed using Wiley, NIST 05 and Adams mass spectra databases (Adams 2007). Quantification of α-farnesene was performed using a pure α-farnesene standard (Payan Bertrand, Grasse, France).

For sterol analysis, around 50 mg DW samples were ground in nitrogen with mortar and pestle. Lipids were extracted and saponified at 80 °C with 15 ml of 6% KOH in methanol for 3 h. Cholesterol was added as internal standard (1.5 mg/gDW). Then, 5 ml of water is added to the mixture and sterols were extracted with tree volumes of hexane. Organic layers were dried using a rotavapor at 30 °C and acylation reaction was performed overnight at room temperature, on the dried residue dissolved in toluene, using pyridine/acetic anhydride (6:4, v/v). Steryl acetates were isolated on a preparative thin-layer chromatography (PLC silica gel 60 0.5 mm, Merck) developed in dichloromethane. Phytosterol analyses were performed on Thermo TRACE GC ultra coupled with a flame ionization detector and equipped with a 30 m × 0.25 mm DB5 apolar capillary column. Injector temperature was at 220 °C and detector at 300 °C. Nitrogen was used as the carrier gas at a flow rate of 1.0 ml/min. Oven temperature settings were: 60 °C at injection, maintained 50 s and followed by a 30 °C/min temperature ramp from 60 to 200 °C, then 15 °C/min from 200 to 300 °C. Temperature

was then kept on hold at 300 °C for 30 min. Campesterol, stigmasterol and β-sitosterol were identified and quantified using pure standards (Extrasynthese). It can be noticed that apple tree naturally produce traces of cholesterol. The use of cholesterol as internal standard does not impact the quantification of main phytosterols, but prevents accurate quantification of endogenous cholesterol.

Triterpene content of around 20 mg of freeze-dried samples ground in nitrogen was extracted three times with 1 ml methanol, incubated for 1 h in a sonication bath. Glycyrrhetinic acid was used as internal standard (0.75 mg/gDW). Supernatants were combined, clarified at 13,000*g* for 5 min and concentrated in speed-vac. Ursolic acid was quantified as the main apple tree triterpene identified, using an HPLC system composed of a Waters 600 controller, an autosampler (Waters 717 plus) and a UV–visible photodiode array detector (Waters 996) controlled by Empower 2 software. Analyses were performed on a column packed with 3 µm particles (250 × 4 mm, Multospher 120 RP18HP; CS-Service, Langerwehe, Germany) at 24 °C. The separation was isocratically undertaken with a solvent consisting of 0.1% (v/v) aqueous phosphoric acid–acetonitrile (75:25, v/v) at a flow rate of 0.5 ml/min during 60 min. Quantification was performed using an ursolic acid pure standard (Extrasynthese).

Results

Malus domestica genome harbors a couple of *SQS* resulting from a recent gene duplication event

Apple tree genome was browsed to identify loci corresponding to putative *SQS*. BLAST searches were performed using sequences of several characterized plant SQS (Fig. 2). Two candidates were found at locus tags MDP0000309694 on chromosome 17 and MDP0000311820 on chromosome 10. Reannotation of the predicted genes was needed to improve sequence retrieval. Our alternative gene predictions were further confirmed by coding sequence (CDS) cloning from cDNA. These sequences of 1239 and 1233 nucleotides are registered in GenBank as Md*SQS1* and Md*SQS2* with the respective accession numbers KC895979 and KC895980. Both genes display 13 exons, and share 96% nucleotide identity and 94.5% at the protein level. As illustrated in the phylogenetic tree generated after alignment of protein sequences (Fig. 2), MdSQSs strongly clustered together compared to characterized SQSs of other species, which may indicate a recent gene duplication event in the apple tree genome. This analysis also highlighted that such duplication events are species dependent.

Both MdSQS1 and MdSQS2 sequences contain all highly conserved SQS domains (Suppl. Fig. S3): A and B

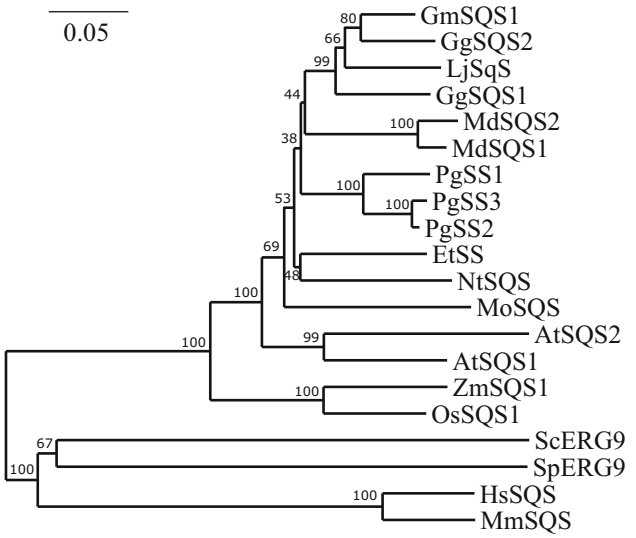

Fig. 2 Phylogenetic tree of putative *M. domestica* SQS compared to a selection of previously characterized squalene synthases from various species. The tree was constructed by neighbor-joining distance analysis on protein sequences. *Line lengths* indicate the relative distances between nodes. *M. domestica* MdSQS1 (KC895979) and MdSQS2 (KC895980); *A. thaliana* AtSQS1 (NP_195190) and AtSQS2 (NP_195191); *M. officinalis* MoSQS (KT223496); *N. tabacum* NtSQS (AAB08578); *P. ginseng* PgSS1 (AB010148), PgSS2 (GQ468527) and PgSS3 (AB115496); *L. japonicus* LjSqS (AB102688); *E. tirucalli* EtSS (AB433916); *G. glabra* GgSQS1 (D86409) and GgSQS2 (D86410); *Glycine max* GmSQS1 (NP_001236365); *Oryza sativa* OsSQS1 (NM_001058160); *Zea mays* ZmSQS1 (NM_001111369); *Saccharomyces pombe* SpERG9 (NP_595363); *S. cerevisiae* ScERG9 (ACD03847); *Mus musculus* MmSQS (BAA06102); *Homo sapiens* HsSQS (CAA48896)

domains shared with phytoene synthase (Summers et al. 1993), an SQS-specific C domain which forms a hydrophobic tunnel interacting with FPP and containing Phe and Gln residues required for enzyme activity (Gu et al. 1998), a flap motif that protects the hydrophobic tunnel, two DxxxD motifs for magnesium dependent binding of NADPH co-factor and, finally, a D domain at C-terminal end, which includes a predicted transmembrane helix to anchor the enzyme to the membrane. Unsurprisingly, the D domains of MdSQS1 and MdSQS2 are the most divergent part of the protein compared to others SQS. As previously reported, D domains and transmembrane sequences are highly variable among SQSs from plants or animals and are also significantly shorter than in yeast (Suppl. Fig. S3).

MdSQS1 and MdSQS2 are two active isoforms of SQS

To assess the activity of MdSQS1 and MdSQS2, both sequences were tested for yeast *erg9* mutant complementation (Kim et al. 2011). The *S. cerevisiae erg9* mutant strain (2C1) is deficient in SQS activity resulting in

ergosterol auxotrophy and cell death. To rescue cell growth, yeasts were transformed with the expression vector pYES2 harboring the full-length coding sequence of Md*SQS1* or Md*SQS2*, but also Sc*ERG9* as a positive control (Fig. 3a). In a first series of experiments, we were unable to complement the *erg9* mutation using either Md*SQS1* or Md*SQS2*. However, the absence of *erg9* complementation was previously observed for few plants and mammals yet active SQS enzymes (Robinson et al. 1993; Kribii et al. 1997). It was proposed that an interaction domain around the SQS transmembrane domain was interacting and channeling with downstream yeast enzymes from the pathway to ensure ergosterol synthesis. Indeed, the SQS transmembrane domain which is quite different between kingdoms as mentioned previously (Suppl. Fig. S3) may impact a metabolon implement. We thus replaced the apple tree SQS transmembrane domain by the equivalent region of ScERG9, but unfortunately the expression of the apple tree chimeric proteins (MdSQS1^{ScTM} and MdSQS2^{ScTM}) did not rescue the cell growth (Fig. 3a).

Although an appropriate membrane anchor is needed for successful yeast complementation, it does not impair enzyme activity in vitro (Kribii et al. 1997). Alternatively, yeast *erg9* mutant strains transformed to express Md*SQS1* or Md*SQS2* were selected and grown on ergosterol-complemented medium. By this way, SQS activity was tested in vitro directly on crude extract with farnesyl diphosphate and NADPH. Squalene production was monitored by TLC (Fig. 3b) and further confirmed by GC using authentic standards. While no squalene was detected on TLC for the reaction mix without enzyme and for reaction mix with crude extract of yeast transformed with empty vector, a clear signal was observed with yeast mutant strain complemented with the Sc*ERG9* expressing plasmid. More importantly, a substantial squalene synthesis was also obtained for crude extracts of yeast expressing Md*SQS1* or Md*SQS2*. However, *M. domestica* SQSs may only lead to low rates of squalene production in yeast, which is probably limiting for a sufficient ergosterol production for yeast growth. Nevertheless, in vitro activities clearly demonstrated the presence of two active SQS isoforms in apple tree.

Subcellular localization of MdSQS1 and MdSQS2

Squalene synthase is reported to function as ER-anchored enzymes. A transmembrane C-terminal hydrophobic α-helix was found in the D domain of each characterized SQS but highly diverging in amino acid sequence between species (Suppl. Fig. S3). Therefore, the localization of apple tree SQS isoforms was investigated using an N-terminal yellow fluorescent protein (YFP) fusion protein

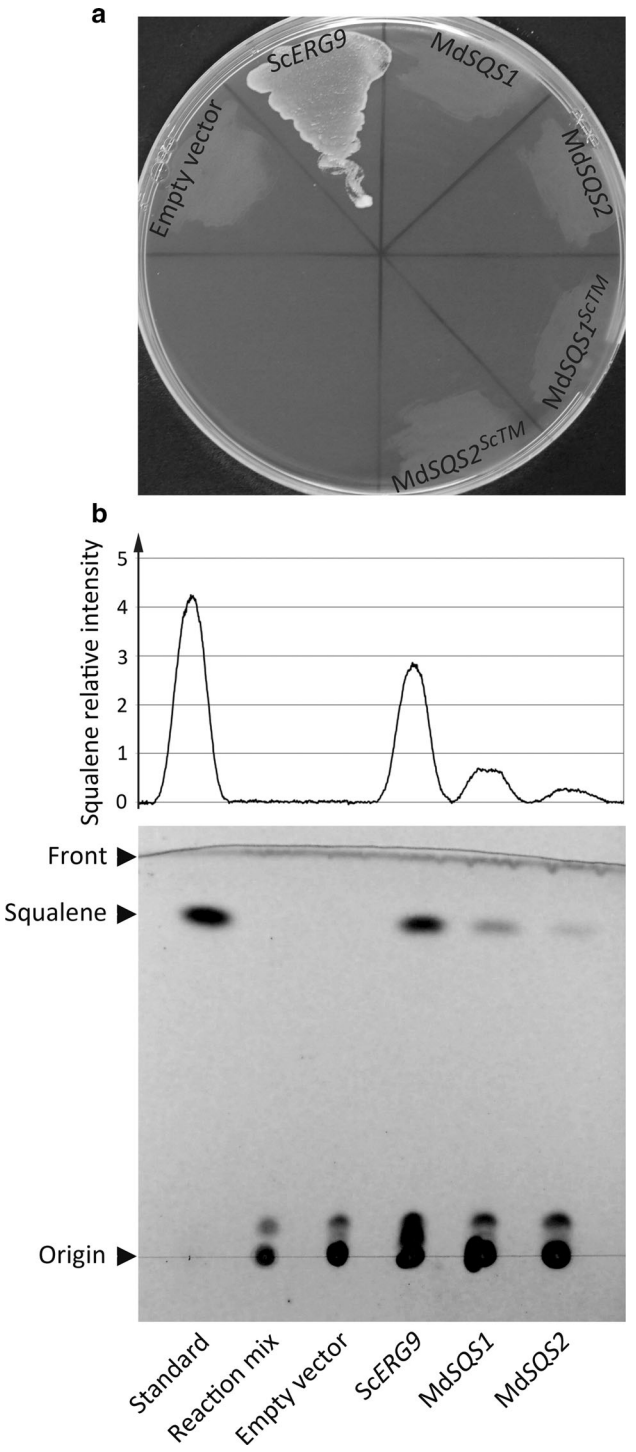

Fig. 3 Characterization of MdSQS1 and MdSQS2 activities. **a** Functional complementation of *S. cerevisiae erg9* mutant strain 2C1, lacking SQS activity, by ScERG9, MdSQS1, MDSQS2 or chimeric transmembrane variants MdSQS1^{ScTM} and MdSQS2^{ScTM} on YPGal medium and incubated for 5 days at 30 °C. **b** TLC analysis of the reaction products of Erg9, MdSQS1 and MdSQS2. Farnesyl diphosphate and NADPH were incubated with the different yeast crude extracts. Authentic squalene was used as standard. *Upper part* shows densitometry-based relative quantification of squalene

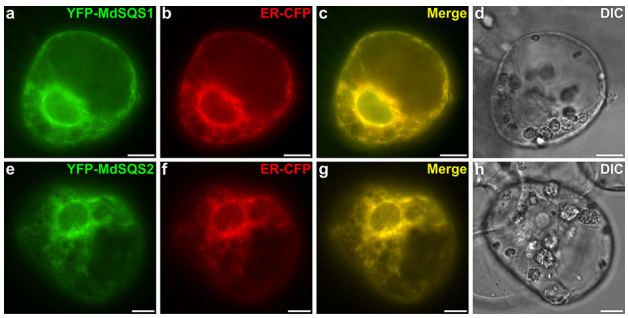

Fig. 4 Subcellular localization of MdSQS1 and MdSQS2. *C. roseus* cells were transiently transformed with YFP-MdSQS1 (**a**) or YFP-MdSQS2 (**e**) expressing vector, in addition to a plasmid expressing an ER-CFP marker (**b**, **f**). Co-localization of the two fluorescence signals appears on the merged images (**c**, **g**). Cell morphology (**d**, **h**) was observed with differential interference contrast (DIC). *Bars* 10 µm

expressed in transiently transformed *C. roseus* cells (Guirimand et al. 2009). The fluorescence signals of YFP-MdSQS1 and YFP-MdSQS2 (Fig. 4a, e) were observed around the nucleus, branching throughout the cell and perfectly superimposed with the signal of the ER-CFP marker (Fig. 4b, c, f, g). Thus, both apple tree SQSs are likely to be anchored to the endoplasmic reticulum membrane as expected and probably facing to the cytosol.

MdSQS isoforms display distinct expression patterns

Distribution of Md*SQS1* and Md*SQS2* transcripts among apple tree organs was investigated by quantitative RT-PCR. Total apple tree *SQS* transcripts (Md*SQS1* + Md*SQS2*) and Md*SQS1*/Md*SQS2* transcript ratios among each condition were measured separately and condensed in Fig. 5a. Total *SQS* transcripts accumulated equally in seedlings, roots and stems. In comparison, transcripts accumulated fourfold higher in leaves and threefold lower in flowers. While both Md*SQS1* and Md*SQS2* were expressed in all organs, Md*SQS1*/Md*SQS2* ratios displayed dramatic differences with a predominance of Md*SQS1* in roots and flowers, representing, respectively, 70 and 90% of *SQS* transcripts and inversely a predominance of Md*SQS2* in stems and leaves representing, respectively, 70 and 80% of *SQS* transcripts (Fig. 5a).

To assess potential variations of gene expression through environmental constraint, *SQS* expression level was investigated after abiotic stress (Fig. 5b, c). First, cold treatment led to a 12-fold transient increase of *SQS* transcripts at 24 h, which was maintained at 48 h and decreased up to the basal level at 72 h (Fig. 5b). Whereas Md*SQS2* transcripts were predominant in control leaves compared to Md*SQS1*, both were up-regulated under cold stress and reached almost equivalent transcript ratios.

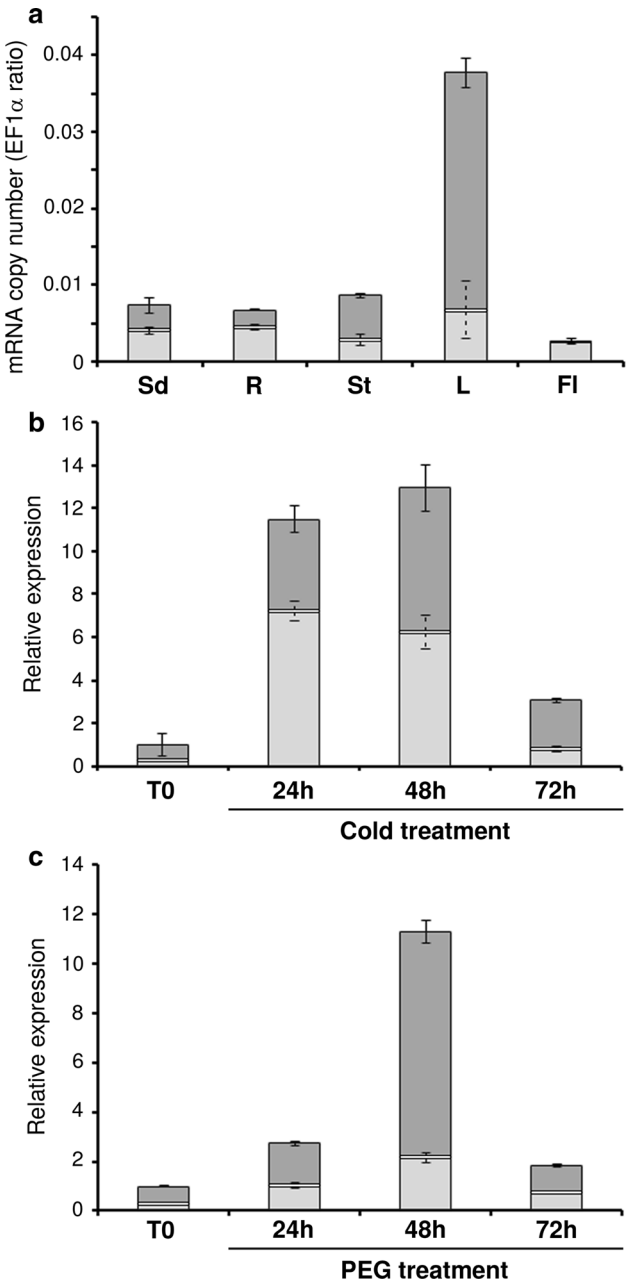

Fig. 5 Analysis of apple tree *SQS* expression pattern. Combined Md*SQS1* and Md*SQS2* transcript levels (total *SQS* transcripts) were measured by RT-qPCR in various organs (**a**) and in leaves subjected to cold (**b**) or PEG-6000 (**c**) treatment. Transcript copy numbers (**a**) and relative expression (**b**, **c**) were normalized using Md*EF1*α. Data correspond to mean values of three samples, each one composed of plant material from three plants. Ratio between Md*SQS1* (*light gray*) and Md*SQS2* (*dark gray*) among total *SQS* transcripts are separated by *double line* on each histogram. Standard deviations for Md*SQS* ratio are indicated in *dot line*. *Sd* seedling, *R* root, *St* stem, *L* leaf, *Fl* flower

Therefore, Md*SQS1* had a more pronounced induction factor (30-fold) than Md*SQS2* (fivefold) under cold treatment. Secondly, to induce and control plant water deficit,

we used PEG6000 treatments. Under hydric stress, *SQS* transcripts displayed the same induction profile as under cold stress. Notably, the 12-fold induction factor was conserved, albeit the increase of *SQS* transcripts was delayed to 48 h. Finally, transcript amounts decreased to basal level at 72 h. In contrast to cold stress, Md*SQS1*/Md*SQS2* ratio of leaves (20/80) remained unchanged all along the experiment. Indeed, Md*SQS1* and Md*SQS2* have an equivalent 12-fold induction factor in response to hydric stress, leading to a predominant expression of Md*SQS2* in these conditions. These results thus suggest that *SQS* expression is induced under abiotic stress to potentially change membrane composition since phytosterol and triterpene contents impact membrane fluidity and stability depending on temperature and osmotic fluctuation.

The differential induction of SQS isoform genes upon stresses as well as their organ-specific ratio addresses the question of their specific involvement in distinct downstream pathway branches leading to phytosterol or triterpene synthesis. Therefore, additional expression analyses were performed through RNAseq data mining (Suppl. Table S2). A total of 310 RNAseq samples were analyzed from EBI ENA for *M. domestica*, regrouping a wide range of conditions including various organs (e.g., roots, shoot apex, cotyledons and seeds), developmental processes (e.g., flowers and fruit development) and stresses (e.g., *Venturia inaequalis* infection). Firstly, the global expression profile of selected triterpene and phytosterol-related genes (Suppl. Table S4) was compared (Fig. 6a) to highlight the overall transcriptional tendencies of each metabolism, according to the usual co-expression of genes involved in a common synthesis pathway. The expression of triterpene-related genes strongly fluctuated depending on plant organs and environmental constraints whereas phytosterol-related gene expression seemed to be more stable in the same conditions. These divergent profiles supported a weak overlap in the transcriptional regulation of each pathway that may facilitate subsequent gene associations. Therefore, lists of genes co-expressed with Md*SQS1* or Md*SQS2* were generated to identify a potential preferred association of each SQS isoform to downstream biosynthetic branch (Suppl. Table S3). Genes retrieved from this analysis shared a strict co-expression profile with the target gene among every tested condition and a Venn diagram of co-expressed genes was generated (Fig. 6b). Surprisingly, MdSQS isoforms shared only 4 co-expressed genes (HRR <500) confirming strong specificities in their expression profiles and potential distinct roles for both enzymes. In addition, several occurrences of genes involved in triterpene metabolism were found in the gene list co-expressed with Md*SQS1* including the previously characterized α-amyrin synthases MdOSC1/MdOSC3 and the C28 triterpene hydroxylase CYP716A175, which argued for a specific involvement of MdSQS1 in triterpene biosynthesis. On the contrary, none of triterpene or phytosterol-related genes was found to be co-expressed with Md*SQS2*, which might reflect the involvement of MdSQS2 in different metabolism types. On the other hand, it is not excluded that MdSQS2 might also be associated with several metabolisms, including or not triterpene and phytosterol biosynthesis, hiding specific gene correlations during our analyses.

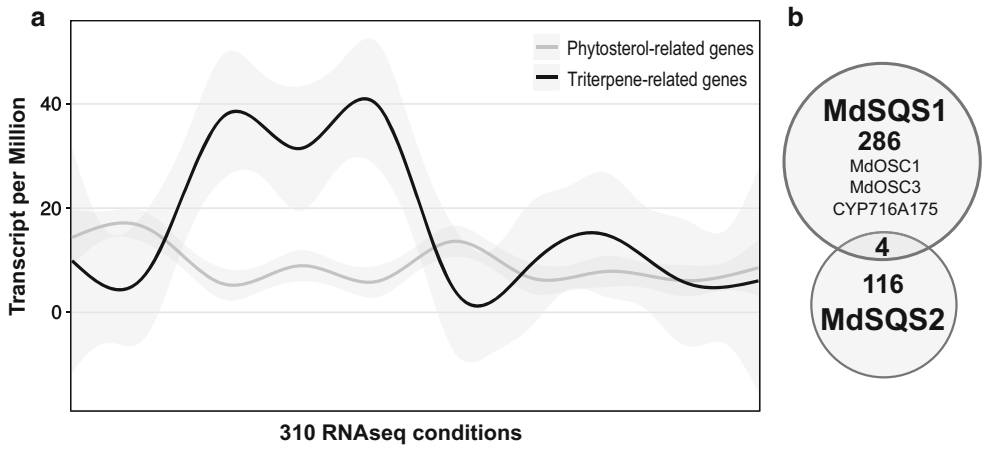

Fig. 6 Determination of co-expressed genes with Md*SQS1* and Md*SQS2* using RNA-seq data. **a** Mean expression profiles of putative triterpene and phytosterol-related genes were compared between 310 conditions of RNA-seq runs available for *M. domestica*. Accession numbers of putative triterpene and phytosterol-related genes are available in Suppl. Fig. S6 and the description of the RNAseq accessions used for the construction of the data matrix is available in Suppl. Fig. S4. **b** Overlap between best co-expressed genes with each apple tree SQS is visualized on a Venn diagram. Lists were established for an HRR <500. Accession numbers of genes found in the co-expression lists are available in Suppl. Fig. S5. The characterized triterpene-related Md*OSC1*, Md*OSC3* and *CYP716A175* found in Md*SQS1* co-expression list are indicated on the diagram

Md*SQS* silencing in apple tree by VIGS leads to abnormal leaves

A virus-induced gene silencing (VIGS) approach was used to investigate the impact of *SQS* down-regulation in apple tree. To significantly abolish the synthesis of squalene in planta, the VIGS assay was designed to target simultaneously Md*SQS1* and Md*SQS2*. To this aim, we generated a modified apple latent spherical virus (ALSV) carrying a 201pb fragment of the Md*SQS1* coding sequence displaying 99% identity with Md*SQS2* and potentially allowing to target both transcripts in planta (Suppl. Fig. S2). The inoculation of this recombinant virus (ALSV-*SQS*) was performed on cotyledons of apple tree seedlings. VIGS establishment and efficiency were monitored by inoculating control plants with a virus targeting the small subunit of ribulose-1,5-bisphosphate carboxylase (ALSV-*rbcS*) whose silencing generates a visual phenotype of leaf chlorosis (Sasaki et al. 2011). Typically, molecular analyses revealed that the first two true leaves contained ALSV even though the targeted genes were not silenced (Suppl. Fig. S4a and b). Gene silencing was observed in the third leaf with an important heterogeneity as the chlorosis phenotype appeared only in one half of the leaves leading to a 54% decrease in *rbcS* global expression. Finally, a full and stable silencing was measured from the fourth leaf (Suppl. Fig. S4a and b). In plants inoculated with ALSV-*SQS*, the third true leaves were falciform (shaped like a sickle) rather than oval, partially albino, smaller than in control plants and displaying various sizes (Fig. 6a), while next leaf development was completely aborted. A 42% decrease in *SQS* expression level was measured in abnormal leaves compared to control plants (Fig. 7b). This *SQS* silencing efficiency is an average and might integrate disparities of VIGS efficiency in the third leaf as observed for *rbcS* (Suppl. Fig. S4b), and explains the heterogeneous phenotype of leaves. Moreover, the absence of fourth leaves potentially revealed the lethality caused by a stronger silencing of *SQS*.

The unexpected falciform and albino phenotypes of the partially silenced *SQS* leaves were further investigated. First, the asymmetric leaf shape in lateral blades (lateral concavity) suggested a difference in tissue development between strong and weakly silenced area. Therefore, surface of palisade parenchyma cells of leaf transversal cross sections was measured on both sides of the central vein (Fig. 8a). Interestingly, cells were slightly but significantly smaller in the concave side of falciform leaves compared to convex side, where cell surface was similar to control leaves (data not shown). However, this weak difference in cell elongation could not explain the pronounced leaf deformation. In addition, the number of cells in the first layer (adjacent to epidermis) of palisade parenchyma was numerated between central vein and leaf margin, on both sides of the *SQS*-silenced leaf (Fig. 8b). We noted an important difference relying on the presence of threefold less cells in the concave side of falciform leaf than in convex side. Therefore, down-regulation of *SQS* expression likely deeply impacts cell division. Secondly, tissues were compared on leaf cross section between green parts and albino spots (Fig. 8c, d). No difference was found in leaf tissue anatomy such as epidermis, palisade or spongy

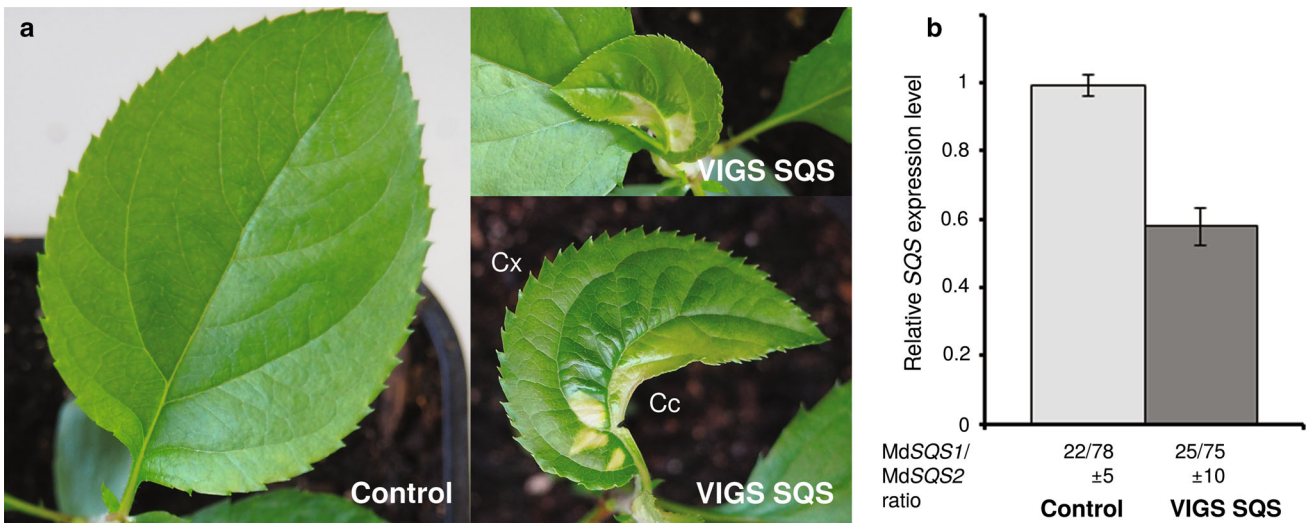

Fig. 7 Down-regulation of *SQS* in apple tree strongly affects plant development. Md*SQS1* and Md*SQS2* were simultaneously targeted by VIGS. **a** Typical leaf phenotypes of VIGS SQS plants are shown and compared with control plants, transformed with ALSV empty construct. **b** Relative *SQS* expression (representing both Md*SQS1* and Md*SQS2*) was measured by RT-qPCR. Ratio between Md*SQS1* and Md*SQS2* among total *SQS* transcripts is indicated under each graphics. Md*EF1*α was used as a reference gene. Data correspond to average values of four samples, each one composed of leaves from ten independent transformed plants. *Cx* convex, *Cc* concave

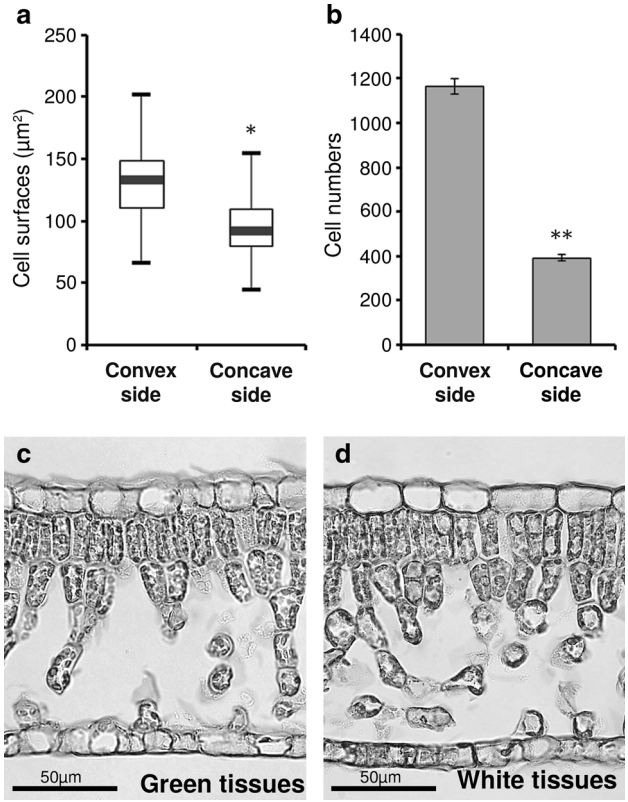

Fig. 8 *SQS* silencing effects on cell leaf anatomy and structure. Surface (**a**) and number (**b**) of palisade cells, observed on cross sections, were compared between convex and concave side of falciform leaves silenced for *SQS*. Plastids are observed on cross section stained with Astra blue. Comparison was made between green tissues (**c**) and white tissues (**d**). *Asterisk* denote statistical significance [$P < 0.0001$ Student's t test, $n = 100$ (**a**) and $n = 6$ (**b**)]

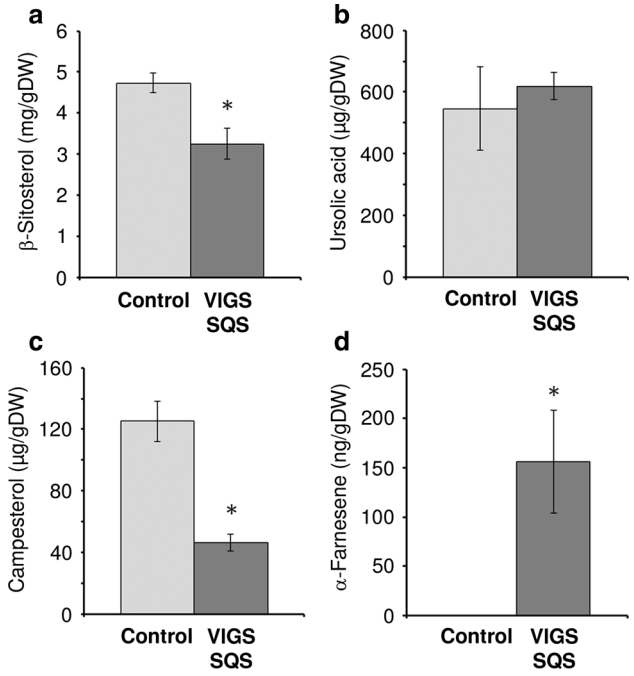

Fig. 9 Sesquiterpene, triterpene and phytosterol contents in *SQS*-silenced leaves compared to control plants. Main compounds of each triterpenoid family were used including β-sitosterol (**a**), ursolic acid (**b**), campesterol (**c**) and α-farnesene (**d**). Standard deviation is representative of 6–9 measurements performed on biological replicates composed of ten leaves. *Asterisk* denotes statistical significance compared to control ($P < 0.001$ Student's t test)

mesophyll cells indicating that cell differentiation occurred properly all through the leaves, independently of *SQS* expression level. Moreover, abundant plastids were observed in parenchyma cells even in albino tissues, with similar size and quantity compared to green parts. Interestingly, the albino phenotype can be attributed to the depigmentation of chloroplast in SQS-silenced leaves rather than a loss of plastids ultrastructure.

SQS-silencing disturbs terpenoid metabolism

Changes in terpene accumulation were studied in *SQS* knock-down leaves by quantification of the main metabolites produced downstream of SQS in the biosynthetic pathway such as ursolic acid and β-sitosterol as the major triterpene and phytosterol in apple tree, respectively (Fig. 1). Ursolic acid levels were similar in leaves of plants silenced for *SQS* and control plants while, in contrast, β-sitosterol contents were significantly lower in *SQS*-silenced leaves (Fig. 9a, b). Campesterol—a phytosterol intermediate in brassinolide biosynthesis—was also quantified. Campesterol contents decreased as observed for β-sitosterol, but in a stronger manner. *SQS*-silenced leaves only accumulated 37% of control plant campesterol (Fig. 9c). Finally, since sesquiterpene synthases and SQS share FPP as substrate, measurements of sesquiterpene contents were also performed. In control plant leaves, sesquiterpene amounts did not reach detection level, whilst α-farnesene was clearly accumulated in *SQS*-silenced leaves (Fig. 9d). In addition, low amounts of germacrene D were sporadically detected in few SQS-silenced plants (data not shown). Taken together, these results clearly showed the importance of SQS in phytosterol production and probably on subsequent brassinolide synthesis; however, no impact was found on triterpene synthesis. Finally, down-regulation of *SQS* seemed to increase the FPP pool available in planta for alternative terpene pathways such as sesquiterpene biosynthesis.

Reduced triterpenoid accumulation in *SQS*-silenced leaves promotes the expression of terpene biosynthetic enzymes

Since triterpenoid is a fine-tuned metabolism, the effects of *SQS*-silencing and the resulting metabolic perturbations were investigated by analyzing the expression of branch

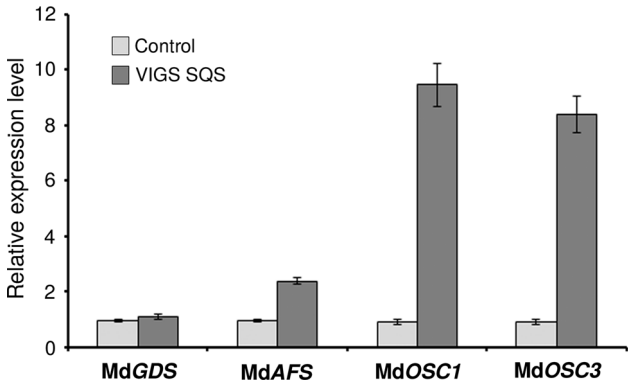

Fig. 10 Effect of *SQS* silencing on sesquiterpene synthase and oxidosqualene cyclase expression levels measured by RT-qPCR. Relative expression levels of Md*GDS* (germacrene D synthase), Md*AFS* (α-farnesene synthase), Md*OSC1* and Md*OSC3* (α-amyrin synthases) in *SQS*-silenced leaves were compared to control plants and normalized with Md*EF1*α. Data correspond to mean values of four samples, each one composed of leaves from ten independent transformed plants

point oxidosqualene cyclases (OSC) including the two previously characterized apple tree α-amyrin synthases Md*OSC1* and Md*OSC3* (Fig. 10) (Brendolise et al. 2011). Interestingly, both genes displayed an important upregulation in *SQS*-silenced plants with eightfold more transcripts compared to control plants. The lake in *SQS* expression seems to act positively on expression of OSC dedicated to triterpene synthesis. Sterol-branch specific OSC such as CAS has still not been characterized in apple tree and could not be included in the present analysis. Otherwise, the expression levels of two sesquiterpene synthases (Nieuwenhuizen et al. 2013) were also measured since α-farnesene and germacrene D transcripts were detected in silenced plants (Fig. 10). A 2.5-fold increase of α-farnesene synthase (Md*AFS*) and no difference for germacrene D synthase (Md*GDS*) were observed. Taken together, these observations show that reduced triterpenoid accumulation in *SQS*-silenced leaves clearly promotes the expression of triterpene biosynthetic enzymes, while weakly impacts the sesquiterpene biosynthetic enzymes.

Discussion

Squalene synthase is an essential enzyme for eukaryotic cells, catalyzing FPP condensation to form squalene. In this study, we demonstrated that apple tree contains two functional SQS isoforms (Fig. 3). *SQS* gene copy number is heterogeneous in higher plants. Similar to apple tree, four other plant species were reported to contain at least two SQS isoforms (Devarenne et al. 1998; Hayashi et al. 1999; Suzuki et al. 2002; Kim et al. 2011). However, some plants species were also found to harbor only one *SQS* gene as in mammals and yeast (Hata et al. 1997; Huang et al. 2007; Uchida et al. 2009). Therefore, *SQS* duplication events in plants seem to be recent and to have occurred in a species-specific manner. This hypothesis is reinforced by the higher identities between SQS isoforms within species than those of SQS orthologues (Fig. 2).

Both MdSQS isoforms are membrane-bound enzymes, anchored in ER (Fig. 4), which confirms the conservation and functionality of the C-terminal transmembrane domain in the apple tree enzymes. However, full-length coding sequences of Md*SQS1* and Md*SQS2* failed to complement the ergosterol synthesis pathway in the *erg9* yeast mutant. This phenomenon, already observed in several other complementation experiments with plant SQS, was previously circumvented by replacement of the plant SQS transmembrane domain by the equivalent region from the yeast enzyme (Kribii et al. 1997). However, such approach did not lead to complementation for apple tree SQS (Fig. 3). The squalene synthesis activity of MdSQS1 and MdSQS2 was finally demonstrated in vitro using yeast crude extracts (Fig. 3). In our conditions, activity of apple tree enzymes was clearly lower than wild-type yeast SQS (Erg9). Therefore, the absence of yeast complementation even with apple tree SQS enzymes modified in their C-terminal domain may be the consequence of a weak intrinsic activity in yeast system. Beyond the confirmation of apple tree SQS functionality, these results raise the question of the limits of yeast *erg9* complementation method to identify active SQS enzymes since it might easily generate false-negative results.

Phytosterol and triterpene biosynthesis both originate from the common precursor 2,3-oxidosqualene whose synthesis requires SQS activity (Fig. 1). However, for both pathways, differences in tissue location exist (Wegel et al. 2009), most probably depending on end-product functions. Genes related to sterol biosynthesis are expressed constitutively throughout the plant since phytosterols are essential for plant growth and development (Clouse 2002; Lindsey et al. 2003). On the contrary, triterpenes act as protective compounds against biotic stresses (González-Coloma et al. 2011), and are differentially accumulated in plant tissues such as in apple skin and leaf cuticle wax (Bringe et al. 2006; Jäger et al. 2009). Therefore, such compartmentalization of specialized metabolism could explain the differential expression profiles observed in our global triterpene and phytosterol-related gene expression analysis (Fig. 6a). Furthermore, the emergence of SQS isoforms in apple tree seems to have been followed by a divergence in their expression and a differential involvement in downstream biosynthetic pathways (Figs. 5, 6). Md*SQS2* presented the highest expression level in aerial organs and could be the main isoform involved in both triterpene and phytosterol biosynthesis. Albeit our

bioinformatic analyses did not lead to any association to specific metabolism, one could speculate that Md*SQS2* may integrate triterpene and phytosterol-related gene expression profiles leading to a complex and dissimilar expression pattern which could explain the low number of co-expressed genes for Md*SQS2* and the absence of strict occurrences with one or the other downstream pathways. On the contrary, Md*SQS1* was globally less expressed but restricted to triterpene synthesis (Figs. 5, 6). Md*SQS1* could thus correspond to the recently duplicated SQS isoform, which completes MdSQS2 functions. However, all these hypothesis are based on qPCR expression studies and gene co-expression network of Md*SQS1* and Md*SQS2* and would require further additional in vivo characterization.

VIGS approaches were successfully developed in apple tree several years ago (Sasaki et al. 2011) but until now, no study has taken advantage of this strategy to disturb metabolic flux and to investigate the function of metabolic enzymes in planta. This was achieved herein for Md*SQS1* and Md*SQS2*; both isoforms were targeted simultaneously due to high sequence identity. Interestingly, although a plethora of *SQS* was cloned among plants, the use of reverse genetic approaches for in planta SQS functional characterization especially using gene down-regulation is scarce (Manavalan et al. 2012; Wang et al. 2012; Singh et al. 2015). This is probably due to the essential roles played by sterols for cells, the disruption of their biosynthesis resulting in lethality (Novotny and Karst 1994; Babiychuk et al. 2008; Kim et al. 2010). We demonstrated that the use of VIGS method circumvents this problem, especially in apple tree since various levels of silencing efficiency naturally occur in newly developed leaves (Suppl. Fig. S4). While the most SQS-silenced leaves aborted probably due to the lack of sterols, weakly silenced pair of leaves were used for our analysis (Fig. 7). The main counterpart of this incomplete silencing was the production of heterogeneous and partial phenotypes leading to less nuanced metabolite variations (Fig. 9). On the other hand, this study on MdSQS highlights that the use of the ALSV-based VIGS method in apple tree constitutes a powerful tool to achieve fast functional genomics on metabolism of interest and allows characterization of essential genes in planta.

SQS-silencing in apple tree disturbed terpene metabolism with a main impact on phytosterol accumulation but not on triterpene synthesis (Fig. 9). Indeed, the potential low level of squalene resulting from SQS-silencing and consequently reduced amount of 2,3-oxidosqualene seems to positively regulate the expression of triterpene-related *OSC* (Brendolise et al. 2011; Andre et al. 2016) such as Md*OSC1* and Md*OSC3* (Fig. 10). This induced expression might compensate the limiting 2,3-oxidosqualene amount and drains the metabolic flux toward triterpene synthesis instead of phytosterol, thus explaining the absence of significant alteration in triterpene accumulation. Unfortunately, *CAS* genes were not identified yet in apple tree impending the study of the impact of *SQS*-silencing on sterol-specific OSC expression. However, the important differences in relative amounts of phytosterol compared to triterpene in untreated plants (Fig. 9) argue for a naturally higher limiting flux for sterol biosynthesis.

Apple tree is able to produce a large range of sesquiterpenes including α-farnesene and germacrene D (Nieuwenhuizen et al. 2013). Sesquiterpenes are volatile compounds involved in plant defense and produced in response to biotic stresses. Sesquiterpene synthases use FPP as a substrate and, therefore, can compete with SQS and triterpenoid pathways (Fig. 1). In fact, elicitor treatment on parsley and tobacco cell cultures was found to stimulate sesquiterpene synthesis with an additional inhibition effect on SQS activity which is probably needed to get enough metabolic flux available for sesquiterpene fast and efficient production (Vögeli and Chappell 1988; Haudenschild and Hartmann 1995; Devarenne et al. 1998). Therefore, an important change in sesquiterpene synthesis was expected in *SQS*-silenced plants. In spite of a substantial accumulation of sesquiterpenes in silenced plants compared to controls, their total amounts were still poor in comparison of the loss of phytosterols (Fig. 9a, c, d). Natural expression level of sesquiterpene synthases in leaves is limited in the absence of environmental constraint (greenhouse growth) and the weak inductions of Md*AFS* and Md*GDS* in *SQS*-silenced plants (Fig. 10c, d) were probably not sufficient to reroute efficiently metabolic flux trough sesquiterpenes.

Since lower phytosterol amount was the main alteration observed in apple tree *SQS*-silenced leaves (Fig. 9), phenotypic alterations could potentially be attributed to sterol deprivation. A plastid depigmentation (Fig. 8) was previously reported in an *Arabidopsis* T-DNA mutant affected in *CAS1* expression (Babiychuk et al. 2008). CAS1 catalyzes the first enzymatic step specific to phytosterol synthesis, downstream of SQS (Fig. 1). Whereas the knock-out allelic mutations *cas1-2* and *cas1-3* did not allow the generation of viable lines, the knock-down allelic mutation *cas1-1* allowed plant development with albino inflorescence shoots suggesting a role of phytosterol in plastid biogenesis. Leaf bleaching was also observed in tobacco down-regulated for CAS1 using a VIGS approach, confirming the previous result (Gas-Pascual et al. 2014). Even if the chloroplast inner membrane and thylakoids did not contain sterols, they may indirectly disturb chloroplast biogenesis through membrane trafficking with sterol-rich ER. Through our *SQS*-silencing approach, the link between phytosterol depletion and albino phenotype was confirmed by targeting an alternative gene in sterol biosynthesis pathway. In addition to the albino phenotype, falciform leaves were obtained in *SQS*-silenced plants. This falciform phenotype

results from a differential leaf growth on both sides of the central vein (Fig. 8) and may be a consequence from a differential silencing efficiency among the leaf. Developmental alterations are usually observed in brassinosteroid-deficient mutants, characterized by pronounced dwarf phenotype (Schaller 2003). Brassinosteroids are well known to play important roles in the regulation of cell division and elongation (Hu et al. 2000; Miyazawa et al. 2003; Müssig 2005). The strong reduction level of campesterol in *SQS*-silenced leaves (Fig. 9) could explain the observed phenotype since campesterol is the precursor of brassinolide (Fig. 1). However, a direct effect of phytosterol deficiency on cell division cannot be excluded. Indeed, exogenous brassinosteroid treatments were not able to systematically rescue the dwarf phenotype of sterol deficient mutant, indicating a brassinosteroid-independent effect of sterols on development (Schaller 2003).

In summary, the characterization of two *SQS* genes in apple tree brings new insights into the involvement of SQS isoforms in phytosterol and triterpene metabolisms in the green lineage. Furthermore, this study opens the way to metabolic disturbance in apple tree using a VIGS approach for functional characterization in planta. Our results provided additional information towards the function of sterols in apple tree but remained limited for triterpenes. At least five different triterpene-specific OSCs were hitherto identified in apple tree (Brendolise et al. 2011; Andre et al. 2016). Direct and specific down-regulations of these Md*OSC* will be needed to give more insight into the complex metabolic flux balance among triterpenoid biosynthesis, to confirm OSC function in planta, and to understand apple tree triterpenes biological function.

Author contribution statement SNG, CEP, DD, FJ, NP, VC, AL and SB conducted experiments. FL and TDDB achieved bioinformatics analyses. AO, GG, OP, NY, VC, MC participated in the design of the study and interpretation. NGG, BSP, LA, MC assisted in the supervision of this work. SB conceived; supervised, coordinated the work and wrote the manuscript. VC, NP and TDDB revised the article. All authors read and approved the final manuscript.

Acknowledgements The authors wish to thank Dr. Marc Fischer (INRA Colmar) for providing yeast *erg9* strain and Dr. Marie-Noëlle Brisset (INRA Angers) for providing apple tree seeds. We gratefully acknowledge support from the Région Centre-Val de Loire (France) for financing SNG and CEP. DD was financed by a doctoral fellowship from the Région Centre-Val de Loire (France) and the Ministère de l'Enseignement Supérieur et de la Recherche (France).

Compliance with ethical standards

Conflict of interest The authors declare that they have no conflict of interest.

References

Adams RP (2007) Identification of essential oil components by gas chromatography/mass spectrometry. Allured Publishing Corporation, Carol Stream

Andre C, Legay S, Deleruelle A, Nieuwenhuizen N, Punter M, Brendolise C, Cooney JM, Lateur M, Hausman JF, Larondelle Y, Laing W (2016) Multifunctional oxidosqualene cyclases and cytochrome P450 involved in the biosynthesis of apple fruit triterpenic acids. New Phytol 211:1279–1294. doi:10.1111/nph.13996

Babiychuk E, Bouvier-Navé P, Compagnon V, Suzuki M, Muranaka T, Van Montagu M, Kushnir S, Schaller H (2008) Allelic mutant series reveal distinct functions for *Arabidopsis* cycloartenol synthase 1 in cell viability and plastid biogenesis. Proc Natl Acad Sci USA 105:3163–3168. doi:10.1073/pnas.0712190105

Baker CH, Matsuda SP, Liu DR, Corey EJ (1995) Molecular cloning of the human gene encoding lanosterol synthase from a liver cDNA library. Biochem Biophys Res Commun 213:154–160. doi:10.1006/bbrc.1995.2110

Becker DM, Guarente L (1991) High-efficiency transformation of yeast by electroporation. Methods Enzymol 194:182–187. doi:10.1016/0076-6879(91)94015-5

Benveniste P (2002) Sterol metabolism. Arabidopsis Book 1:e0004. doi:10.1199/tab.0004

Brendolise C, Yauk YK, Eberhard ED, Wang M, Chagne D, Andre C, Greenwood D, Beuning LL (2011) An unusual plant triterpene synthase with predominant α-amyrin- producing activity identified by characterizing oxidosqualene cyclases from *Malus* × *domestica*. FEBS J 278:2485–2499. doi:10.1111/j.1742-4658.2011.08175.x

Bringe K, Schumacher CF, Schmitz-Eiberger M, Steiner U, Oerke E (2006) Ontogenetic variation in chemical and physical characteristics of adaxial apple leaf surfaces. Phytochemistry 67:161–170. doi:10.1016/j.phytochem.2005.10.018

Busquets A, Keim V, Closa M, Del Arco A, Boronat A, Arró M, Ferrer A (2008) *Arabidopsis thaliana* contains a single gene encoding squalene synthase. Plant Mol Biol 67:25–36. doi:10.1007/s11103-008-9299-3

Clouse SD (2002) *Arabidopsis* mutants reveal multiple roles for sterols in plant development. Plant Cell 14:1995–2000. doi:10.1105/tpc.140930

Corey EJ, Matsuda SPT, Bartel B (1993) Isolation of an *Arabidopsis thaliana* gene encoding cycloartenol synthase by functional expression in a yeast mutant lacking lanosterol synthase by the use of a chromatographic screen. Proc Natl Acad Sci USA 90:11628–11632

D'Abrosca B, Fiorentino A, Monaco P, Pacifico S (2005) Radical-scavenging activities of new hydroxylated ursane triterpenes from cv. Annurca apples. Chem Biodivers 2:953–958. doi:10.1002/cbdv.200590072

Devarenne TP, Shin DH, Back K, Yin S, Chappell J (1998) Molecular characterization of tobacco squalene synthase and regulation in response to fungal elicitor. Arch Biochem Biophys 349:205–215. doi:10.1006/abbi.1997.0463

Dugé de Bernonville T, Guyot S, Paulin JP, Gaucher M, Loufrani L, Henrion D, Derbré S, Guilet D, Richomme P, Dat JF, Brisset MN (2010) Dihydrochalcones: implication in resistance to oxidative stress and bioactivities against advanced glycation end-products and vasoconstriction. Phytochemistry 71:443–452. doi:10.1016/j.phytochem.2009.11.004

Eberhardt MV, Lee CY, Liu RH (2000) Antioxidant activity of fresh apples. Nature 405:903–904. doi:10.1038/35016148

Elejalde-Palmett C, Dugé de Bernonville T, Glévarec G, Pichon O, Papon N, Courdavault V, St-Pierre B, Giglioli-Guivarc'H N, Lanoue A, Besseau S (2015) Characterization of a spermidine hydroxycinnamoyltransferase in *Malus domestica* highlights the evolutionary conservation of trihydroxycinnamoyl spermidines in pollen coat of core Eudicotyledons. J Exp Bot 66:7271–7285. doi:10.1093/jxb/erv423

Gas-Pascual E, Berna A, Bach TJ, Schaller H (2014) Plant oxidosqualene metabolism: cycloartenol synthase–dependent sterol biosynthesis in *Nicotiana benthamiana*. PLoS One 9:e109156. doi:10.1371/journal.pone.0109156

González-Coloma A, López-Balboa C, Santana O, Reina M, Fraga BM (2011) Triterpene-based plant defenses. Phytochem Rev 10:245–260. doi:10.1007/s11101-010-9187-8

Goodstein DM, Shu S, Howson R, Neupane R, Hayes RD, Fazo J, Mitros T, Dirks W, Hellsten U, Putnam N, Rokhsar DS (2012) Phytozome: a comparative platform for green plant genomics. Nucleic Acids Res 40:1178–1186. doi:10.1093/nar/gkr944

Gu P, Ishii Y, Spencer TA, Shechter I (1998) Function-structure studies and identification of three enzyme domains involved in the catalytic activity in rat hepatic squalene synthase. J Biol Chem 273:12515–12525. doi:10.1074/jbc.273.20.12515

Guirimand G, Burlat V, Oudin A, Lanoue A, St-Pierre B, Courdavault V (2009) Optimization of the transient transformation of *Catharanthus roseus* cells by particle bombardment and its application to the subcellular localization of hydroxymethylbutenyl 4-diphosphate synthase and geraniol 10-hydroxylase. Plant Cell Rep 28:1215–1234. doi:10.1007/s00299-009-0722-2

Hartmann M-A (1998) Plant sterols and the membrane environment. Trends Plant Sci 3:170–175. doi:10.1016/S1360-1385(98)01233-3

Hata S, Sanmiya K, Kouchi H, Matsuoka M, Yamamoto N, Izui K (1997) cDNA cloning of squalene synthase genes from mono- and dicotyledonous plants and expression of the gene in rice. Plant Cell Physiol 38:1409–1413. doi:10.1093/oxfordjournals.pcp.a029137

Haudenschild C, Hartmann M-A (1995) Accumulation of furanocoumarins in parsley cell suspension cultures. Phytochemistry 40:1117–1124. doi:10.1016/0031-9422(95)00434-9

Hayashi H, Hirota A, Hiraoka N, Ikeshiro Y (1999) Molecular cloning and characterization of two cDNAs for *Glycyrrhiza glabra* squalene synthase. Biol Pharm Bull 22:947–950

He X, Rui HL (2007) Triterpenoids isolated from apple peels have potent antiproliferative activity and may be partially responsible for apple's anticancer activity. J Agric Food Chem 55:4366–4370. doi:10.1021/jf063563o

Herrera JBR, Bartel B, Wilson WK, Matsuda SP (1998) Cloning and characterization of the *Arabidopsis thaliana* lupeol synthase gene. Phytochemistry 49:1905–1911. doi:10.1016/S0031-9422(98)00366-5

Ho SN, Hunt HD, Horton RM, Pullen JK, Pease LR (1989) Site-directed mutagenesis by overlap extension using the polymerase chain reaction. Gene 77:51–59. doi:10.1016/0378-1119(89)90358-2

Hu Y, Bao F, Li J (2000) Promotive effect of brassinosteroids on cell division involves a distinct CycD3-induction pathway in *Arabidopsis*. Plant J 24:693–701. doi:10.1046/j.1365-313X.2000.00915.x

Huang Z, Jiang K, Pi Y, Hou R, Liao Z, Cao Y, Han X, Wang Q, Sun X, Tang K (2007) Molecular cloning and characterization of the yew gene encoding squalene synthase from *Taxus cuspidata*. J Biochem Mol Biol 40:625–635

Jäger S, Trojan H, Kopp T, Laszczyk MN, Scheffler A (2009) Pentacyclic triterpene distribution in various plants—rich sources for a new group of multi-potent plant extracts. Molecules 14:2016–2031. doi:10.3390/molecules14062016

Jennings SM, Tsay YH, Fisch TM, Robinson GW (1991) Molecular cloning and characterization of the yeast gene for squalene synthetase. Proc Natl Acad Sci USA 88:6038–6042

Kim HB, Lee H, Oh CJ, Lee HY, Eum HL, Kim HS, Hong YP, Lee Y, Choe S, An C, Choi SB (2010) Postembryonic seedling lethality in the sterol-deficient *Arabidopsis cyp51A2* mutant is partially mediated by the composite action of ethylene and reactive oxygen species. Plant Physiol 152:192–205. doi:10.1104/pp.109.149088

Kim T-D, Han J-Y, Huh GH, Choi Y-E (2011) Expression and functional characterization of three squalene synthase genes associated with saponin biosynthesis in *Panax ginseng*. Plant Cell Physiol 52:125–137. doi:10.1093/pcp/pcq179

Kolesnikova MD, Xiong Q, Lodeiro S, Hua L, Matsuda SPT (2006) Lanosterol biosynthesis in plants. Arch Biochem Biophys 447:87–95. doi:10.1016/j.abb.2005.12.010

Kribii R, Arró M, Del Arco A, González V, Balcells L, Delourme D, Ferrer A, Karst F, Boronat A (1997) Cloning and characterization of the *Arabidopsis thaliana SQS1* gene encoding squalene synthase—involvement of the C-terminal region of the enzyme in the channeling of squalene through the sterol pathway. Eur J Biochem 249:61–69. doi:10.1111/j.1432-1033.1997.00061.x

Kushiro T, Shibuya M, Ebizuka Y (1998) Cloning of oxidosqualene cyclase that catalyzes the formation of the most popular triterpene among higher plants. Eur J Biochem 256:238–244

Lee MH, Jeong JH, Seo JW, Shin CG, Kim YS, In JG, Yang DC, Yi JS, Choi YE (2004) Enhanced triterpene and phytosterol biosynthesis in *Panax ginseng* overexpressing squalene synthase gene. Plant Cell Physiol 45:976–984. doi:10.1093/pcp/pch126

Lindsey K, Pullen ML, Topping JF (2003) Importance of plant sterols in pattern formation and hormone signalling. Trends Plant Sci 8:521–525. doi:10.1016/j.tplants.2003.09.012

Ma CM, Cai SQ, Cui JR, Wang RQ, Tu PF, Hattori M, Daneshtalab M (2005) The cytotoxic activity of ursolic acid derivatives. Eur J Med Chem 40:582–589. doi:10.1016/j.ejmech.2005.01.001

Manavalan LP, Chen X, Clarke J, Salmeron J, Nguyen HT (2012) RNAi-mediated disruption of squalene synthase improves drought tolerance and yield in rice. J Exp Bot 63:163–175. doi:10.1093/jxb/err258

Mckenzie TL, Jiang G, Straubhaar JR, Conrad DG, Shechters I (1992) Molecular cloning, expression, and characterization of the cDNA for the rat hepatic squalene synthase. J Biol Chem 267:21368–21374

Miyazawa Y, Nakajima N, Abe T, Sakai A, Fujioka S, Kawano S, Kuroiwa T, Yoshida S (2003) Activation of cell proliferation by brassinolide application in tobacco BY-2 cells: effects of brassinolide on cell multiplication, cell-cycle-related gene expression, and organellar DNA contents. J Exp Bot 54:2669–2678. doi:10.1093/jxb/erg312

Müssig C (2005) Brassinosteroid-promoted growth. Plant Biol 7:110–117. doi:10.1055/s-2005-837493

Mutwil M, Klie S, Tohge T, Giorgi FM, Wilkins O, Campbell MM, Fernie AR, Usadel B, Nikoloski Z, Persson S (2011) PlaNet: combined sequence and expression comparisons across plant networks derived from seven species. Plant Cell 23:895–910. doi:10.1105/tpc.111.083667

Nelson BK, Cai X, Nebenführ A (2007) A multicolored set of in vivo organelle markers for co-localization studies in *Arabidopsis* and other plants. Plant J 51:1126–1136. doi:10.1111/j.1365-313X.2007.03212.x

Nieuwenhuizen NJ, Green SA, Chen X, Bailleul EJD, Matich AJ, Wang MY, Atkinson RG (2013) Functional genomics reveals that a compact terpene synthase gene family can account for terpene volatile production in apple. Plant Physiol 161:787–804. doi:10.1104/pp.112.208249

Novotny C, Karst F (1994) Sterol dependent growth and ethanol tolerance of a sterol-auxotrophic *erg9:HIS3* mutant of *Saccharomyces cerevisiae*. Biotechnol Lett 16:539–542. doi:10.1007/BF01023340

Pandit J, Danley DE, Schulte GK, Mazzalupo S, Pauly T, Hayward CM, Hamanaka ES, Thompson JF, Harwood HJ (2000) Crystal structure of human squalene synthase. Biochemistry 275:30610–30617. doi:10.1074/jbc.M004132200

Patro R, Duggal G, Love MI, Irizarry RA, Kingsford C (2016) Salmon provides accurate, fast, and bias-aware transcript expression estimates using dual-phase inference. Preprint BioarXiv. doi:10.1101/021592

Pechous SW, Whitaker BD (2004) Cloning and functional expression of an (E, E)-farnesene synthase cDNA from peel tissue of apple fruit. Planta 219:84–94. doi:10.1007/s00425-003-1191-4

Phillips DR, Rasbery JM, Bartel B, Matsuda SP (2006) Biosynthetic diversity in plant triterpene cyclization. Curr Opin Plant Biol 9:305–314. doi:10.1016/j.pbi.2006.03.004

Racovita RC, Jetter R (2016) Composition of the epicuticular waxes coating the adaxial side of *Phyllostachys aurea* leaves: identification of very-long-chain primary amides. Phytochemistry 130:1–10. doi:10.1016/j.phytochem.2016.06.005

Robinson GW, Tsay YIMH, Kienzle BK, Smith-monroy CA, Bishop RW (1993) Conservation between human and fungal squalene synthetases: similarities in structure, function, and regulation. Mol Cell Biol 13:2706–2717. doi:10.1128/MCB.13.5.2706

Sasaki S, Yamagishi N, Yoshikawa N (2011) Efficient virus-induced gene silencing in apple, pear and japanese pear using *Apple latent spherical virus* vectors. Plant Methods 7:15–25. doi:10.1186/1746-4811-7-15

Schaller H (2003) The role of sterols in plant growth and development. Prog Lipid Res 42:163–175. doi:10.1016/S0163-7827(02)00047-4

Schaller H (2004) New aspects of sterol biosynthesis in growth and development of higher plants. Plant Physiol Biochem 42:465–476. doi:10.1016/j.plaphy.2004.05.012

Seo JW, Jeong JH, Shin CG, Lo SC, Han SS, Yu KW, Harada E, Han JY, Choi YE (2005) Overexpression of squalene synthase in *Eleutherococcus senticosus* increases phytosterol and triterpene accumulation. Phytochemistry 66:869–877. doi:10.1016/j.phytochem.2005.02.016

Shi Z, Buntel CJ, Griffin JH (1994) isolation and characterization of the gene encoding 2,3-oxidosqualene- lanosterol cyclase from *Saccharomyces cerevisiae*. Proc Natl Acad Sci USA 91:7370–7374

Singh AK, Dwivedi V, Rai A, Pal S, Reddy SGE, Rao DKV, Shasany AK, Nagegowda D (2015) Virus-induced gene silencing of *Withania somnifera* squalene synthase negatively regulates sterol and defence-related genes resulting in reduced withanolides and biotic stress tolerance. Plant Biotechnol J 13:1287–1299. doi:10.1111/pbi.12347

Sonawane PD, Pollier J, Panda S, Szymanski J, Massalha H, Yona M et al (2016) Plant cholesterol biosynthetic pathway overlaps with phytosterol metabolism. Nat Plants 3:16205–16218. doi:10.1038/nplants.2016.205

Summers C, Karst F, Charles AD (1993) Cloning, expression and characterisation of the cDNA encoding human hepatic squalene synthase, and its relationship to phytoene synthase. Gene 136:185–192. doi:10.1016/0378-1119(93)90462-C

Suzuki H, Achnine L, Xu R, Matsuda SPT, Dixon R (2002) A genomics approach to the early stages of triterpene saponin biosynthesis in *Medicago truncatula*. Plant J 32:1033–1048. doi:10.1046/j.1365-313X.2002.01497.x

Suzuki M, Xiang T, Ohyama K, Seki H, Saito K, Muranaka T, Van Montagu M, Kushnir S, Schaller H (2006) Lanosterol synthase in dicotyledonous plants. Plant Cell Physiol 47:565–571. doi:10.1093/pcp/pcj031

Uchida H, Yamashita H, Kajikawa M, Ohyama K, Nakayachi O, Sugiyama R, Yamato KT, Muranaka T, Fukuzawa H, Takemura M, Ohyama K (2009) Cloning and characterization of a squalene synthase gene from a petroleum plant, *Euphorbia tirucalli L.* Planta 229:1243–1252. doi:10.1007/s00425-009-0906-6

Velasco R, Zharkikh A, Affourtit J, Dhingra A, Cestaro A, Kalyanaraman A et al (2010) The genome of the domesticated apple (*Malus* × *domestica* Borkh.). Nat Genet 42:833–839. doi:10.1038/ng.654

Vincken JP, Heng L, de Groot A, Gruppen H (2007) Saponins, classification and occurrence in the plant kingdom. Phytochemistry 68:275–297. doi:10.1016/j.phytochem.2006.10.008

Vögeli U, Chappell J (1988) Induction of sesquiterpene cyclase and suppression of squalene synthetase activities in plant cell cultures treated with fungal elicitor. Plant Physiol 88:1291–1296. doi:10.1104/pp.88.4.1291

Wang Z, Guhling O, Yao R, Li F, Yeats TH, Rose JKC, Jetter R (2011) Two oxidosqualene cyclases responsible for biosynthesis of tomato fruit cuticular triterpenoids. Plant Physiol 155:540–552. doi:10.1104/pp.110.162883

Wang K, Senthil-Kumar M, Ryu C-M, Kang L, Mysore KS (2012) Phytosterols play a key role in plant innate immunity against bacterial pathogens by regulating nutrient efflux into the apoplast. Plant Physiol 158:1789–1802. doi:10.1104/pp.111.189217

Wang W, Bai MY, Wang ZY (2014) The brassinosteroid signaling network-a paradigm of signal integration. Curr Opin Plant Biol 21:147–153. doi:10.1016/j.pbi.2014.07.012

Wegel E, Koumproglou R, Shaw P, Osbourn A (2009) Cell type-specific chromatin decondensation of a metabolic gene cluster in oats. Plant Cell 21:3926–3936. doi:10.1105/tpc.109.072124

Zhang H, Dugé de Bernonville T, Body M, Glévarec G, Reichelt M, Unsicker S, Bruneau M, Renou JP, Huguet E, Dubreuil G, Giron D (2016) Leaf-mining by *Phyllonorycter blancardella* reprograms the host-leaf transcriptome to modulate phytohormones associated with nutrient mobilization and plant defense. J Insect Physiol 84:114–127. doi:10.1016/j.jinsphys.2015.06.003